NeuroImage 47 (2009) 1545–1557

Contents lists available at ScienceDirect

NeuroImage

journal homepage: www.elsevier.com/locate/ynimg

Increased sensitivity to effects of normal aging and Alzheimer's disease on cortical thickness by adjustment for local variability in gray/white contrast: A multi-sample MRI study

Lars T. Westlye [a,*], Kristine B. Walhovd [a,b], Anders M. Dale [c,d,e], Thomas Espeseth [a], Ivar Reinvang [a], Naftali Raz [f], Ingrid Agartz [g,h,i], Douglas N. Greve [j], Bruce Fischl [j,k], Anders M. Fjell [a,b]

[a] Center for the Study of Human Cognition, Department of Psychology, University of Oslo, Oslo 0317, Norway
[b] Department of Neuropsychology, Ullevaal University Hospital, Oslo 0407, Norway
[c] Multimodal Imaging Laboratory, University of California, San Diego, CA 92103, USA
[d] Department of Radiology, University of California, San Diego, CA 92103, USA
[e] Department of Neurosciences, University of California, San Diego, CA 92103, USA
[f] Department of Psychology and Institute of Gerontology, Wayne State University, Detroit, MI 48201, USA
[g] Department of Psychiatric Research, Diakonhjemmet Hospital, Oslo 0319, Norway
[h] Department of Psychiatry, University of Oslo, Oslo 0319, Norway
[i] Human Brain Informatics (HUBIN), Department of Clinical Neuroscience, Psychiatry Section, Karolinska Institutet and Hospital, SE-171 76 Stockholm, Sweden
[j] Athinoula A. Martinos Center, Department of Radiology, Massachusetts General Hospital, Harvard Medical School, Boston, MA 02129, USA
[k] Massachusetts Institute of Technology, Computer Science and Artificial Intelligence Laboratory, Cambridge, MA 02139, USA

ARTICLE INFO

Article history:
Received 30 March 2009
Revised 21 May 2009
Accepted 26 May 2009
Available online 6 June 2009

ABSTRACT

MRI-based estimates of cerebral morphometric properties, e.g. cortical thickness, are pivotal to studies of normal and pathological brain changes. These measures are based on automated or manual segmentation procedures, which utilize the tissue contrast between gray and white matter on T_1-weighted MR images. Tissue contrast is unlikely to remain a constant property across groups of different age and health. An important question is therefore how the sensitivity of cortical thickness estimates is influenced by variability in WM/GM contrast. The effect of adjusting for variability in WM/GM contrast on age sensitivity of cortical thickness was tested in 1189 healthy subjects from six different samples, enabling evaluation of consistency of effects within and between sites and scanners. Further, the influence of Alzheimer's disease (AD) diagnosis on cortical thickness with and without correction for contrast was tested in an additional sample of 96 patients. In healthy controls, regional increases in the sensitivity of the cortical thickness measure to age were found after correcting for contrast. Across samples, the strongest effects were observed in frontal, lateral temporal and parietal areas. Controlling for contrast variability also increased the cortical thickness estimates' sensitivity to AD, thus replicating the finding in an independent clinical sample. The results showed increased sensitivity of cortical estimates to AD in areas earlier reported to be compromised in AD, including medial temporal, inferior and superior parietal regions. In sum, the findings indicate that adjusting for contrast can increase the sensitivity of MR morphometry to variables of interest.

Introduction

Stable and predictable changes in brain structure in healthy aging and Alzheimer's disease (AD) are documented by MRI studies (Allen et al., 2005; Fjell et al., in press; Ikram et al., in press; Jernigan et al., 2001; Raz et al., 2005; Raz and Rodrigue, 2006; Raz et al., 2004b; Resnick et al., 2000, 2003; Salat et al., 2004; Sowell et al., 2003; Thompson et al., 2007, 2004; Walhovd et al., 2009a, 2005, in press-b). Any MRI segmentation procedure is ultimately dependent on the contrast in signal intensity between gray (GM) and white (WM) matter. To the extent that age affects the WM/GM contrast, this could invalidate the observed age effects. Further, observed heterogeneity of age effects across the cortical mantle could be explained by regional differences in contrast. The present study was designed to test 1) whether age affects WM/GM contrast and 2) to what extent controlling for variability in contrast influences estimated age effects on cortical thickness and increases the effects of Alzheimer's disease (AD). Since large studies typically include multiple sites and scanners (e.g. *Alzheimer's Disease Neuroimaging Initiative*, http://www.adni-info.org/), we tested these effects with a large multi-site dataset.

Most brain morphometric studies are based on T_1-weighted MR scans. Partly due to differences in T_1 relaxation times between tissues, WM appears brighter than GM, making it feasible to separate the

* Corresponding author. Fax: +4722845001
E-mail address: l.t.westlye@psykologi.uio.no (L.T. Westlye).

1053-8119/$ – see front matter © 2009 Elsevier Inc. All rights reserved.
doi:10.1016/j.neuroimage.2009.05.084

tissue classes based on intensity information. While some current segmentation approaches (e.g. Freesurfer, (Dale and Sereno, 1993; Dale et al., 1999; Fischl et al., 1999a) and other automated tissue classification procedures (Cocosco et al., 2003; de Boer et al., 2009; Vrooman et al., 2007)) do not depend simply on WM/GM contrast alone, this information is invariably critical to any manual or automated segmentation procedure. The contrast in T_1 signal reflects neurobiological differences related to cell water and lipid content of the tissues. Aging and disease affects both the amount and structure of the myelin layer covering neuronal WM axons (Peters, 2002) and perhaps to a lesser degree, the cortical neuronal architecture (Pakkenberg and Gundersen, 1997; Piguet et al., 2009). Cellular changes such as myelin degradation affect the magnetic properties of cerebral tissues (Cho et al., 1997; Ogg and Steen, 1998; Raz et al., 1990; Steen et al., 1997), giving rise to a decrease in tissue contrast along the WM/GM border. This reduction in contrast could lead to a less valid representation of the tissue border with increasing age (Raz and Rodrigue, 2006) or disease. Further, these alterations in signal intensity show regional variability (Imon et al., 1998; Ogg and Steen, 1998). Tissue contrast is also affected by scanner and sequence parameters (Han et al., 2006; Jack et al., 2008), and although several multi-sample studies and cross-scanner validations have been published (Fennema-Notestine et al., 2007; Fjell et al., in press; Han et al., 2006; Jovicich et al., 2009; Pardoe et al., 2008; Walhovd et al., 2009a, in press-a), the effect of site-dependent and between-subject variance in tissue contrast on age or diagnostic sensitivity has not been directly assessed.

In the present study, a novel procedure for adjusting estimated thickness for local WM/GM contrast on T_1-weighted MRI volumes was used. Surface-based analyses of the age effects on both thickness and contrast were employed. Regional age sensitivity was compared between contrast adjusted and non-adjusted thickness data. Effects in composite measures like ratios may be caused by changes in one or both measures, so we further tested whether age-related alterations in WM/GM contrast were best described in terms of WM or GM signal intensity alterations. To address this question, contrast and intensity values sampled at seven different distances along the WM/GM border were mapped to a common surface and the sensitivity was compared over sampling distances across the surface. 1189 healthy subjects from six different samples scanned on six different scanners from two different vendors were included in the present study, enabling evaluation of consistency of age effects within and between site and scanner. An additional sample of 96 AD patients from one of the six sites was included to test if correcting for contrast variability increases diagnostic sensitivity, thus addressing the clinical utility of the proposed procedure.

Materials and methods

Samples

The demographic details of each of the six healthy samples are described in Table 1 with key publications and selection criteria noted. The samples are overlapping with that of Fjell et al. (in press) except that sample 4 and the AD sample were added to the present study. The total number of included healthy participants was 1189 (58.8% females), with an age range of 75 years (18–93 years). Data for the AD versus controls analyses were drawn from the Open Access Series of Imaging Studies database (OASIS) (http://www.oasis-brains.org/). 96 AD subjects were included in the present study (mean age 76.6 years, range 62–96 years, 59% females). 93 healthy and age matched subjects (mean age 76.7 years, range 61–94, 74% females) were selected from the OASIS database to populate the control group. Education was higher in the control group ($p<.05$), with 3.3 vs 2.8 points (2: high school, 3: some college, 4: college grad.). Socio-economic status did not differ significantly between groups (2.8 in AD vs 2.5 in controls, where a high degree indicates low status). Mean MMSE score was significantly lower ($p<.05$) (mean 24.4, range 14–30) in AD than controls (mean 28.9, range 25–30). Earlier studies sampling from this database have contrasted AD patients with healthy controls (Buckner et al., 2005; Dickerson et al., 2009b; Fotenos et al., 2008; Fotenos et al., 2005; Salat et al., 2009). Recruitment, screening and MR acquisition details are described in depth elsewhere (Marcus et al., 2007). All subjects underwent the Alzheimer's Disease Research Center's full clinical assessment, yielding clinical dementia rating (CDR) for all participants (Berg, 1988). A global CDR of 0 was taken to indicate absence of dementia, and CDR of 0.5 or higher to indicate mild to moderate AD. Other active neurological or psychiatric illnesses, serious head injury, history of clinically significant stroke, use of psychoactive drugs and gross anatomical anomalies detected on MR were exclusion criteria.

All subjects gave their informed consent following the different institutions` guidelines, and were screened for history of neurological conditions. Although preclinical pathological processes cannot be

Table 1

Sample	Country	*N* (% f)	Age mean (range)	Education mean (range)	Key publications	Main screening instruments/inclusion criteria
1	SWE	106 (32)	41.6 (19–56)	14 (9–22)	Jonsson et al. (2006); Nesvag et al. (2008)	Health interview, DSM-III-R, WASI vocabulary>16[a]
2	NOR	69 (57)	51.3 (20–88)	15 (7–20)	Walhovd et al. (2005)	Health interview, MMSE>26, BDI<16, IQ>85, RH only
3	NOR	208 (71)	46.8 (19–75)	14 (9–22)	Espeseth et al. (2006); Espeseth et al. (2008)	Health interview, IQ>85
4	NOR	306 (56)	50.3 (20–93)	16[c] (8–22)	Fjell et al. (2008b); Westlye et al. (2009)	Health interview, MMSE>26[b], BDI<16[c], IQ>85[c], RH only, neuroradiology
5	USA	309 (63)	44.5 (18–94)	3.5 (1–5)[d]	Marcus et al. (2007)	Health interview, CDR=0[e], MMSE>25[e], RH only
6	USA	191 (60)	47.3 (18–81)	15.7 (12–21)	Raz et al. (2004a)	Health interview, BIMCT>30, GDQ<15, RH only, neuroradiology

Nor: Norway.
Swe: Sweden.
% f: percentage of female participants.
MMSE: Mini Mental Status Exam (Folstein et al., 1975).
BDI: Beck Depression Inventory (Beck and Steer, 1987).
BIMCT: Blessed Information-Memory-Concentration Test (Blessed et al., 1968).
CDR: Clinical Dementia Rating (Berg, 1984, 1988; Morris, 1993).
GDQ: Geriatric Depression Questionnaire (Auer and Reisberg, 1997).
RH: Right handed.
WASI: Wechsler Abbreviated Scale of Intelligence (Wechsler, 1999).
[a] Available for 70 participants.
[b] Available for participants >40 years.
[c] Available for 305 participants.
[d] Available for all participants ≥60 years, and sporadically for the rest. 1: less than high school grad., 2: high school grad., 3: some college, 4: college grad., 5: beyond college.
[e] Available for participants ≥60 years only.

Table 2
MRI parameters.

Sample	Vendor/model	MRI protocol
Sample 1	General Electric Signa	One 3D spoiled gradient recalled (SPGR) pulse T1-weighted sequence TR/TE/FA = 24 ms/6.0 ms/35°, number of excitations was 2 Matrix: 256 × 192 Each volume consisted of 1.5 mm coronal slices, no gap, FOV = 24 cm
Sample 2	Siemens Symphony Quantum	Two 3D magnetization prepared rapid gradient-echo (MP-RAGE) T1-weighted sequences TR/TE/TI/FA = 2730 ms/4 ms/1000 ms/7° Matrix = 192 × 256 Scan time: 8.5 min per volume. Each volume consisted of 128 sagittal slices (1.33 × 1 × 1 mm).
Sample 3	Siemens Sonata	Two 3D magnetization prepared rapid gradient-echo (MP-RAGE) T1-weighted sequences TR/TE/TI/FA = 2730 ms/3.43 ms/1000 ms/7° Matrix: 256 × 256 Scan time: 8 min and 46 s per volume Each volume consisted of 128 sagittal slices (1.33 × 1 × 1 mm)
Sample 4	Siemens Avanto	Two 3D magnetization prepared rapid gradient-echo (MP-RAGE) T1-weighted sequences TR/TE/TI/FA = 2400 ms/3.61 ms/1000 ms/8° Matrix: 192 × 192 Scan time: 7 min and 42 s per volume Each volume consisted of 160 sagittal slices (1.25 × 1.25 × 1.20 mm)
Sample 5	Siemens Vision	3–4 individual T1-weighted magnetization prepared rapid gradient-echo (MP-RAGE) T1-weighted sequences TR/TE/TI/FA = 9.7 ms/4.0 ms/20 ms/10° Matrix = 256 × 256. Each volume consisted of 128 sagittal slices (1.25 × 1 × 1 mm).
Sample 6	General Electric Signa	One 3D spoiled gradient recalled (SPGR) pulse T1-weighted sequence TR/TE/FA = 24 ms/5.0 ms/30° Matrix = 256 × 192 Each volume consisted of 124 axial slices w/slice thickness 1.3 mm FOV = 22 cm

FOV: Field of view, FA: Flip angle, TR: Repetition time, TE: Echo time, TI: Inversion time.

ruled out with certainty without extensive medical and neuropsychological evaluations and follow-ups, it is assumed that the reported age effects can be attributed to grossly non-pathological aging processes. 23 participants were excluded due to bad scan quality, including overfolding, MR artefacts, errors during data transfer or saving, converting errors, or deviant signal intensities in the MR volumes. While most of these artefacts were too small to cause disruption of the analyses stream, they were still excluded due to inadequate data quality. Of these 23 subjects were also a small number of participants excluded due to structural WM anomalies. The removal of 23 subjects is not assumed to have biased the data. Four subjects in the AD group were excluded due to less than optimal scan quality, bringing the sample down to 96 included AD patients.

MR acquisition

Details of the sequence parameters used are given in Table 2. The AD datasets were acquired with the same parameters as sample 5. All subjects were scanned at 1.5T, but from two different vendors (Siemens, Erlangen, Germany; General Electric CO. [GE], Milwaukee, WI), and five different models (Siemens Symphony Quantom, Siemens Sonata, Siemens Vision, Siemens Avanto and GE Signa). All samples were scanned on different scanners, but scanner was kept constant within each sample. T_1-weighted 3D magnetization prepared gradient-echo (MP-RAGE) sequences were acquired for the Siemens scanners, and T_1-weighted 3D spoiled gradient recalled (SPGR) pulse sequences for the GE scanners. Slice thickness varied between 1.25 mm and 1.5 mm with acquisition matrices of 192 × 192, 256 × 192 or 256 × 256. In four of the samples (samples 2, 3, 4 and 5), multiple scans were acquired within the same session, and averaged to increase SNR. Examples of the scan quality from five samples (1–3, 5–6) are presented in Fig. 1 in Fjell et al. (in press).

Cortical thickness and WM/GM contrast analyses

All datasets were processed and analysed with Freesurfer 4.05 (http://surfer.nmr.mgh.harvard.edu/) at the Neuroimaging Analysis Lab, Center for the Study of Human Cognition, University of Oslo, with additional use of computing resources from the Titan High Performance Computing facilities (http://hpc.uio.no/index.php/Titan) at the University of Oslo. Measurements of cortical thickness were obtained by reconstructing representations of the WM/GM boundary and the cortical surface (Dale and Sereno, 1993; Dale et al., 1999; Fischl and Dale, 2000; Fischl et al., 2002, 2004a, 1999a,b, 2004b; Segonne et al., 2004, 2005, 2007), and then calculating the distance between these surfaces at each vertex across the cortical mantle. Importantly, the thickness maps are created using spatial intensity gradients across tissue classes and are therefore not simply reliant on absolute signal intensity. The maps are not restricted to the voxel resolution of the original data and are capable of detecting sub-millimeter differences between groups (Fischl and Dale, 2000). This has been validated using histology and MR (Kuperberg et al., 2003; Rosas et al., 2002). The volumes used for intensity calculation were resampled from native resolution to 1 × 1 × 1 mm, zero padded to 256 × 256 × 256 dimension, motion corrected and, where available, averaged over multiple acquisitions yielding one high signal-to-noise ratio (SNR) volume. While the full Freesurfer stream employs a number of normalization procedures prior to the final tissue classification, no further high- or low-frequency intensity normalization was performed on the volumes on which intensity values were computed. Sampling from intensity normalised volumes (i.e. where the different tissue classes are individually scaled to standardised distributions) would probably influence the present results by assuming indifferent mean intensities for each tissue class across subjects. Intensity values used to calculate WM/GM contrast were sampled at a distance of 0.2 mm from the WM/GM boundary (white surface). WM/GM contrast was computed by dividing each vertex' WM value at 0.2 mm from the white surface by the corresponding GM value at 0.2 mm from the white surface and projecting the ratio onto a common surface. Further five sampling distances were included in the WM (0.4, 0.6, 0.8, 1.0 and 1.2 mm) to test for possible age-related effects in WM intensity as a function of distance from the WM surface. The GM values were sampled towards the pial surface and the WM towards the center of the gyri. Each vertex across the mantle was thus represented with an estimated value of cortical thickness, six WM intensity values, one GM value and WM/GM contrast sampled at 0.2 mm towards both sides. To normalize intensities with respect to scanner and sequence related noise, mean ventricle CSF intensity was computed for each subject and included in the models as separate global regressors in addition to sex and sample. An automated subcortical segmentation procedure implemented in Freesurfer (Fischl et al., 2002, 2004a) was used to extract intensity values from the ventricle CSF. To minimize partial voluming effects at the outskirts of the ventricles, all ventricle segments were eroded in all three dimensions by 2 voxels prior to applying them as masks for mean intensity calculation. In addition, by use of an automated surface-based labeling system (Desikan

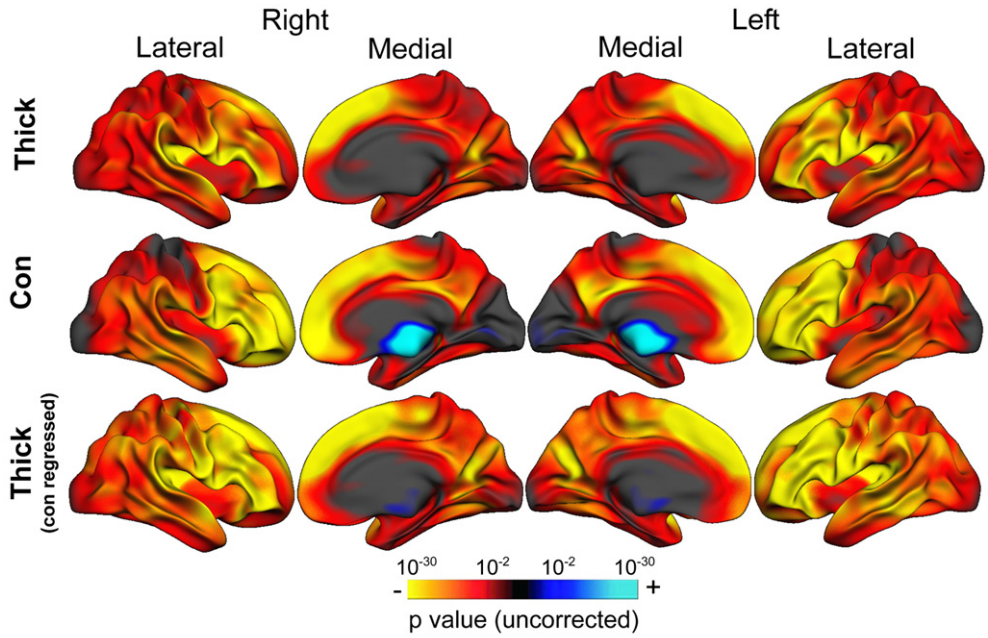

Fig. 1. Adjusting for contrast increases age sensitivity for cortical thickness. Statistical p maps thresholded at $p<10^{-2}$ superimposed on a template brain's semi-inflated surface showing the results from GLMs testing the effect of age on thickness (top row), contrast (middle row) and thickness adjusted for contrast (bottom row). Warm colors denote areas with age-related thinning or contrast decay across samples. Adjusting for contrast increases age sensitivity in large portions of the surface compared to when not adjusting for contrast.

et al., 2006; Fischl et al., 2004b), the cortical surface was divided into 33 different gyral-based areas in each hemisphere. Anatomically distributed ROIs were selected for further statistical testing.

Thickness, intensity and contrast maps were smoothed using a circularly symmetric Gaussian kernel across the surface with a full width at half maximum (FWHM) of 15 mm and averaged across participants using a non-rigid high-dimensional spherical averaging method to align cortical folding patterns (Fischl et al., 1999a). This provides accurate matching of morphologically homologous cortical locations among participants on the basis of each individual's anatomy while minimizing metric distortion, resulting in a measure of interest for each person at each vertex on the reconstructed surface. The surface reconstruction and segmentation procedures are basically run in an automated fashion, but require manual supervision of the accuracy of the spatial registration and the tissue segmentations steps. The types of errors that most often required manual user intervention in the current datasets were insufficient removal of non-brain tissue (typically dura in superior brain areas and vessels adjacent to the cortex, especially in the temporal lobes and orbitofrontal cortices). In addition, in presence of local artefacts, small parts of WM may mistakenly be segmented as GM, thus obscuring the WM/GM boundary. All volumes were visually checked for accuracy, and the types of segmentation errors mentioned above were manually corrected by trained operators. Small manual edits were performed on most (>80%) subjects, usually restricted to removal of vessels orbitofrontally included in the cortical surface. Although the scan quality varied between samples, we do not think the manual interventions biased the present results. It has been argued that manual interventions are not necessary, and that cortical thickness can be estimated reliably across field strength, scanner upgrade and manufacturer without manual interventions (Han et al., 2006). This was not tested in the present study.

Statistical analyses

Regional effects of age and diagnosis on thickness, tissue contrast and intensity were tested by General Linear Models (GLMs) at each vertex. Sex and sample were treated as covariates in all cross sample analyses, and differential age-related slopes per sex and sample were allowed (different intercept and slopes assumed). To estimate the effects of age on the different metrics independently, the vertex-wise values were included as per-vertex-regressors (PVRs) in the GLMs. This allowed for testing the effects of the global regressors while controlling for a vertex-wise measure. It was thus possible to model the regional effects of age or diagnosis on cortical thickness while controlling for WM/GM contrast in the corresponding vertices. As we in an overlapping sample recently found no additional explanatory value in adding the square of age in the models (Fjell et al., in press), we only modelled linear effects of age in the present study. The resulting statistical maps were mapped to a semi-inflated common surface using the correspondence established by the spherical registration. To test the effects of adjusting for local contrast on the age- and diagnosis–thickness relationships, the results from the GLMs with and without PVRs were compared. For both age and AD analyses, thickness and contrast were computed within various cortical regions of interest (ROIs), and the mean values were submitted to linear regressions to estimate the effects of age and diagnosis on thickness when adjusting for contrast and not. In addition to unstandardized and standardized betas, t and p statistics, the squared ratios of the t-scores from the linear regressions with/without contrast are reported as an indicator of effect of contrast adjustment. A squared ratio >1 was taken as an indication of increased power. The significance of changes in effect sizes were tested by t-tests of the standardized betas in selected anatomically distributed ROIs. The ROIs for the AD analyses were selected based on previous studies showing regional cortical thinning in AD in an overlapping sample (Dickerson et al., 2009a). Finally, effects of age on the surface mapped composites of the contrast ratio (signal intensities) were tested with GLMs and plotted as a function of age and sampling distance from the white surface.

Results

Cortical thinning and contrast decay in aging

Results from the GLMs testing age effects on thickness and contrast are displayed in Fig. 1. Warm colors denote areas with significant age-related thinning ($p<.05$). As earlier reported (Fjell et al., in press), strong and wide-spread thinning of the cerebral cortex was observed

across samples (upper row). As evident at the middle row in Fig. 1, age-related contrast decay was observed across large portions of the surface, and was particularly pronounced bilaterally in medial and lateral frontal regions. Strong effects were also observed in the lateral temporal lobes extending into the temporo-parietal junction and inferior parietal regions. In general, there was substantial overlap between areas of cortical thinning and contrast decay.

Adjusting for contrast in thickness analyses of aging

Importantly, age effects on thickness increased when adjusting for contrast (Fig. 1, bottom row as compared to the upper row). 16 ROIs were selected for further statistical analyses. Table 3 shows the ROI results from the linear regressions with and without adjusting for anatomically corresponding contrast. All ROIs tested showed a significant cortical thinning with advancing age. The unstandardized betas indicate estimated thinning in mm per decade before and after regressing out contrast. As evident from the *t*-ratios, an increased power was observed in most ROIs after correcting for contrast. Strongest increases, as indicated by *t*-ratios, were seen bilaterally in the medial orbitofrontal, paracentral, precentral and the entorhinal cortices. Decreases were observed bilaterally in the superior frontal gyrus, superior and middle temporal gyrus, and the right pericalcarine and inferior parietal gyrus. *T*-tests of the difference between the standardized betas indicated significant ($p<.01$) effects of adjusting for contrast in all ROIs except in the right parahippocampal area. Fig. 2 shows estimated betas (indicating age-related thinning scaled to mm per decade) for each independent sample before and after correcting for contrast. Although this does not necessarily reflect increased sensitivity per se or allows for inferences on significance, all samples showed regional increases in unstandardized betas across the surface, indicating relative stability across groups in the effects of adjusting for contrast.

Adjusting for contrast in thickness analyses of AD

Fig. 3 shows the results from the GLMs testing the difference between AD and controls in cortical thickness (upper row). Warm colors denote areas with a relative thinning in AD compared to controls. A characteristic regional pattern of cortical thinning in AD was found in medial temporal areas, precuneus, retrosplenial cortex and anterior portions of the lateral temporal lobes, inferior and superior parietal areas as well as caudal and rostral middle frontal gyri. After adjusting for contrast (Fig. 3, bottom row), the observed effects were regionally enlarged and strengthened, including greater portions of the inferior and superior parietal gyri, the precuneus, medial and lateral frontal and temporal regions. Results from the ROI analyses are given in Table 4. The unstandardized betas indicate mean cortical thinning in AD relative to controls. Of the 32 selected ROIs, 24 initially showed a significant ($p<.05$) difference in thickness between groups. Largest group differences as indicated by beta were found in the entorhinal and right parahippocampal cortices, the inferior, middle and superior temporal and inferior parietal gyri. No significant difference was found bilaterally in paracentral or pericalcarine sulci, in

Table 3
Adjusting for local contrast variability increases age sensitivity.

		Thickness				Thickness (adjusted)				*t*-ratio	R	*p*(diff)
		beta	SB	*t*	*p*	beta	SB	*t*	*p*			
LH	SFG	−.058	−.501	−28.95	***	−.066	−.568	−25.28	***	.76	.898	**
	mOFC	−.023	−.184	−8.06	***	−.041	−.333	−13.25	***	2.70	.902	**
	Paracentral	−.038	−.323	−15.54	***	−.056	−.475	−23.24	***	2.24	.917	**
	Inferior par	−.045	−.435	−22.88	***	−.051	−.491	−23.44	***	1.05	.879	**
	Inferior temp	−.034	−.338	−14.70	***	−.041	−.415	−15.69	***	1.14	.926	**
	Isthmus	−.045	−.387	−15.83	***	−.051	−.441	−16.86	***	1.13	.933	**
	Middle temp	−.043	−.412	−18.77	***	−.049	−.471	−18.18	***	.94	.902	**
	Superior temp	−.065	−.594	−28.36	***	−.069	−.628	−26.23	***	.86	.968	**
	Parahippoc	−.041	−.246	−9.37	***	−.046	−.276	−10.39	***	1.23	.928	**
	Precuneus	−.044	−.434	−22.39	***	−.052	−.512	−23.65	***	1.12	.916	**
	Posterior cing	−.041	−.400	−18.77	***	−.047	−.458	−20.33	***	1.17	.843	**
	Superior par	−.037	−.375	−19.49	***	−.044	−.449	−23.02	***	1.40	.888	**
	Entorhinal	−.038	−.196	−8.02	***	−.044	−.231	−9.47	***	1.40	.999	**
	Lateral occ	−.034	−.395	−18.42	***	−.038	−.436	−21.27	***	1.33	.883	**
	Precentral	−.055	−.473	−25.32	***	−.071	−.618	−29.95	***	1.40	.952	**
	Pericalcarine	−.033	−.375	−19.58	***	−.030	−.349	−19.93	***	1.04	.978	**
RH	SFG	−.056	−.481	−28.60	***	−.065	−.553	−25.41	***	.79	.874	**
	mOFC	−.022	−.175	−8.00	***	−.038	−.305	−12.29	***	2.38	.900	**
	Paracentral	−.044	−.381	−18.68	***	−.060	−.522	−25.10	***	1.81	.898	**
	Inferior par	−.045	−.440	−22.11	***	−.050	−.488	−21.74	***	.97	.892	**
	Inferior temp	−.025	−.223	−10.49	***	−.034	−.297	−12.16	***	1.34	.908	**
	Isthmus	−.046	−.387	−15.97	***	−.055	−.465	−18.55	***	1.35	.936	**
	Middle temp	−.040	−.381	−17.49	***	−.044	−.423	−16.10	***	.85	.900	**
	Superior temp	−.061	−.552	−26.60	***	−.066	−.601	−25.08	***	.90	.952	**
	Parahippoc	−.035	−.226	−8.70	***	−.038	−.244	−9.30	***	1.14	.936	n.s.
	Precuneus	−.045	−.448	−23.14	***	−.053	−.526	−24.56	***	1.13	.926	**
	Posterior cing	−.038	−.360	−17.07	***	−.043	−.409	−17.70	***	1.08	.844	**
	Superior par	−.036	−.367	−19.00	***	−.044	−.450	−22.99	***	1.47	.908	**
	Entorhinal	−.029	−.131	−5.49	***	−.038	−.171	−7.23	***	1.73	.992	**
	Lateral occ	−.036	−.394	−17.50	***	−.040	−.433	−19.66	***	1.26	.923	**
	Precentral	−.052	−.444	−22.93	***	−.072	−.610	−29.72	***	1.68	.953	**
	Pericalcarine	−.031	−.352	−18.16	***	−.027	−.304	−17.55	***	.93	.950	**

The table shows estimated betas indicating mean thinning in cortical thickness (mm) per decade before and after adjusting for contrast. LH: left hemisphere, RH: right hemisphere, SB: standardized beta, *t*: *t* value of the age effect, *p*: significance of the age effect, *t*-ratio: $(t\_adjusted/t\_nonadjusted)^2$, *t*-ratio >1 indicates increased effect size, *p*(diff): significance of the difference in effect size after adjusting for contrast. *R*: Pearson's correlation coefficient between thickness and thickness after regressing out contrast in each ROI. *R* was used in the *t*-tests testing the significance of the change in effect size after adjusting for contrast.
n.s.: not significant.
* $p<.05$.
** $p<.001$.
*** $p<.0001$.

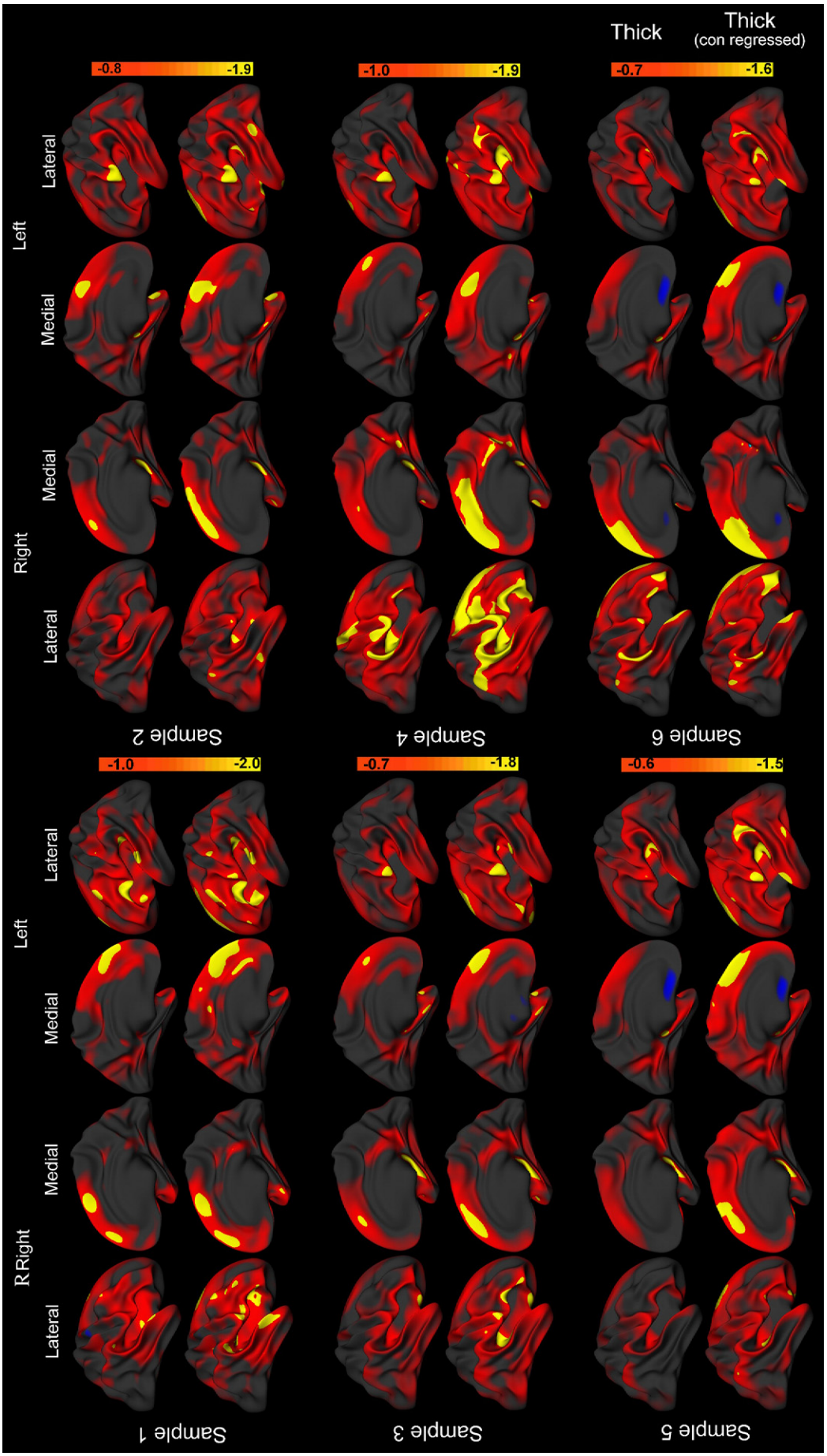

Fig. 2. Adjusting for contrast increases estimated age-related cortical thinning in all samples. Vertex-wise unstandardized betas (mm × 10^{-1} per decade) mapped to a common surface. For within sample comparison purposes, the scale differs between samples. Warmer colors denote steeper negative regression slope, blue denotes age-related thickening, seen in the subgenual area of sample 5 and 6. As estimates of residual variance are not accounted for here, an increase or decrease in estimated beta does not necessarily reflect significant changes in age-related cortical thinning.

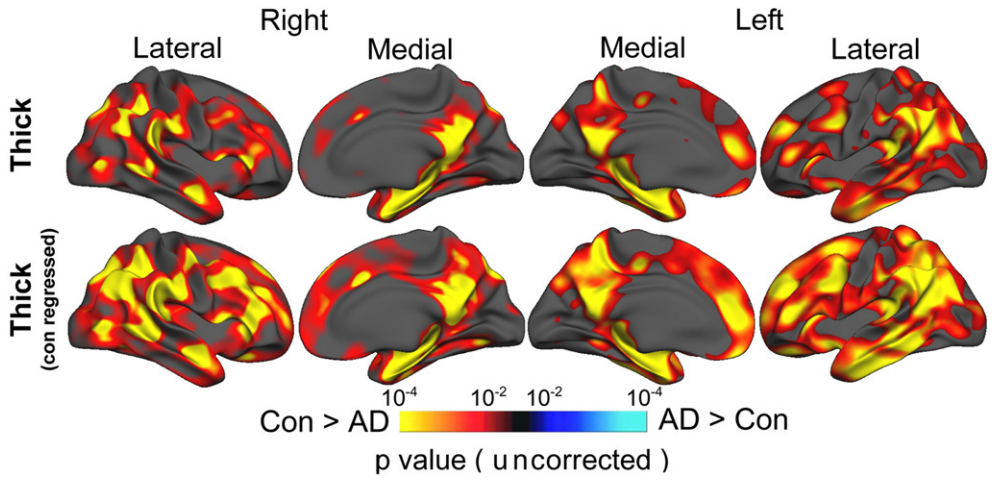

Fig. 3. Adjusting for contrast increases AD sensitivity for cortical thickness. Statistical p maps thresholded at $p<10^{-2}$ superimposed on a template brain's semi-inflated surface showing the results from GLMs testing the difference between AD and controls. Warm colors denote areas with significantly thinner cortex in AD compared to controls while blue colors indicate the opposite relation. Adjusting for contrast (lower row) increases sensitivity for AD over large portions of the brain compared to when not adjusting for contrast (upper row).

the left parahippocampal or in the left posterior cingulate cortex. As evident in Fig. 3 (bottom row), regionally increased effects were observed after controlling for contrast. This was confirmed in the ROI analyses. The results after contrast correction yielded significant group differences in the left parahippocampal and the left paracentral region, and 30 of 32 ROIs showed a relative increase in power as indexed by the a t-ratio > 1. Decreases in power were found bilaterally in the entorhinal cortices, but this area still yielded the largest difference in thickness between groups, as indicated by beta. Among the areas showing a significant group difference, the largest relative

Table 4
Adjusting for local variability in contrast increases sensitivity for AD.

		Thickness				Thickness (adjusted)				t-ratio	R	p(diff)
		beta	SB	t	p	beta	SB	t	p			
LH	SFG	.070	.255	3.61	***	.078	.286	4.03	***	1.25	n.t.	n.t.
	mOFC	.051	.145	2.02	.045	.065	.186	2.99	.003	2.97	n.t.	n.t.
	Paracentral	.036	.108	1.52	.130	.048	.144	2.16	.032	2.01	n.t.	n.t.
	Inferior par	.098	.335	4.88	***	.105	.360	5.21	***	1.14	.999	**
	Inferior temp	.109	.299	4.28	***	.123	.336	4.75	***	1.23	.996	**
	Isthmus	.118	.323	4.66	***	.122	.336	5.12	***	1.21	.954	n.s.
	Middle temp	.106	.309	4.45	***	.114	.333	4.68	***	1.11	.999	**
	Superior temp	.093	.261	3.84	***	.095	.269	3.90	***	1.03	.999	**
	Parahippoc	.084	.137	1.88	.061	.094	.152	2.08	.039	1.22	n.t.	n.t.
	Precuneus	.081	.283	4.11	***	.090	.315	4.66	***	1.29	n.t.	n.t.
	Posterior cing	.028	.092	1.27	.207	.037	.119	1.76	.080	1.93	n.t.	n.t.
	Superior par	.070	.224	3.23	**	.079	.251	3.89	***	1.45	.957	n.s.
	Entorhinal	.272	.307	4.52	***	.248	.279	4.01	***	.79	.967	**
	Lateral occ	.034	.137	1.98	.049	.038	.151	2.20	.029	1.23	n.t.	n.t.
	Precentral	.048	.161	2.29	.023	.064	.214	3.15	.002	1.89	n.t.	n.t.
	Pericalcarine	.015	.060	.86	.392	.013	.053	.88	.381	1.05	n.t.	n.t.
RH	SFG	.061	.216	3.03	.003	.068	.242	3.36	**	1.23	n.t.	n.t.
	mOFC	.062	.166	2.31	.022	.081	.215	3.23	**	1.95	n.t.	n.t.
	Paracentral	.017	.059	.81	.417	.034	.118	1.82	.071	4.98	n.t.	n.t.
	Inferior par	.092	.319	4.72	***	.100	.345	5.05	***	1.14	.999	**
	Inferior temp	.085	.251	3.53	**	.108	.317	4.45	***	1.59	.985	**
	Isthmus	.121	.298	4.27	***	.136	.335	5.01	***	1.37	.975	*
	Middle temp	.071	.222	3.10	.002	.078	.243	3.26	**	1.11	.999	**
	Superior temp	.106	.311	4.60	***	.113	.330	4.86	***	1.11	.999	**
	Parahippoc	.138	.249	3.51	**	.159	.287	4.00	***	1.30	n.t.	n.t.
	Precuneus	.079	.263	3.88	***	.086	.286	4.26	***	1.21	n.t.	n.t.
	Posterior cing	.055	.177	2.47	.014	.062	.199	2.96	.003	1.43	n.t.	n.t.
	Superior par	.083	.262	3.81	***	.090	.283	4.46	***	1.37	.949	n.s.
	Entorhinal	.295	.359	5.29	***	.265	.323	4.59	***	.75	.970	*
	Lateral occ	.066	.231	3.47	**	.068	.241	3.65	***	1.11	n.t.	n.t.
	Precentral	.064	.219	3.10	.002	.075	.259	3.88	***	1.56	n.t.	n.t.
	Pericalcarine	.003	.012	.16	.870	.011	.045	.76	.449	21.34	n.t.	n.t.

The table shows estimated beta indicating mean difference in cortical thickness (mm) between AD and controls before and after adjusting for contrast. Positive values indicate thinner cortex in AD. LH: left hemisphere, RH: right hemisphere, SB: standardized beta, t: t value of the group difference, p: significance of the group difference, t-ratio: (t_adjusted/t_nonadjusted)^2, t-ratio >1 indicates increased effect size, n.t.: not tested, p(diff): significance of the difference in effect size after adjusting for contrast. R: Pearson's correlation coefficient between thickness and thickness after regressing out contrast in each ROI. R was used in the t-tests testing the significance of the change in effect size after adjusting for contrast. This was tested in selected ROIs known to be affected by AD.
n.s.: not significant.
* $p<.05$.
** $p<.001$.
*** $p<.0001$.

increases in power were found bilaterally in the mOFC, the paracentral regions (right hemisphere not significantly related to AD), posterior cingulate (right hemisphere not significantly related to AD), precentral, inferior temporal and superior parietal regions. To test the significance of the changes in effect sizes, standardized betas from seven bilateral ROIs earlier reported to be affected by AD (inferior parietal, inferior temporal, isthmus cingulate, middle temporal, superior temporal, superior parietal, entorhinal) were submitted to statistical analyses. Of the 14 bilateral ROIs, 9 showed a significant ($p<.05$) increase in effect size (L/R inferior parietal, L/R inferior temporal, R isthmus, L/R middle temporal and L/R superior temporal), two showed a significant decrease (L/R entorhinal) and 3 showed no evidence ($p>.05$) of changed effect sizes (L isthmus and L/R superior parietal).

ROI analyses: thickness, contrast and aging

For comparison over samples 1–6, results from ROI based correlation analyses between mean thickness and age and between mean contrast and age per sample are given in Supplementary Tables 1 and 2. Key results are briefly noted here. Both thickness and contrast showed significant bilateral negative age-related associations in most ROIs. The results supported the vertex based GLMs suggesting large and wide-spread negative correlations with age, with some exceptions. For tissue contrast, the lateral occipital and lingual cortices showed significant or trend negative effects of age in all samples except sample four, where trend (lateral occipital) and significant (lingual) positive correlations with age were found. Similar patterns were observed in the post central and pericalcarine cortices. The overall regional pattern of age-related thinning and contrast decay was relatively consistent across samples. Pearsons's correlations between thickness and contrast in each ROI before and after partialling out age are given in Supplementary Table 3 and Supplementary Table 4 for each sample. The results generally showed large regional variability, and no evidence of a uniform relationship between thickness and tissue contrast was found.

Surface-based analyses: WM and GM signal intensity and age

Effects on WM/GM contrast could reflect changes in either WM or GM signal intensity, or both. Fig. 4 shows the results from GLMs testing the effects of age on signal intensities at different sampling distances from the white surface. Significant regional decay (blue areas) in signal intensity with advancing age was found in several

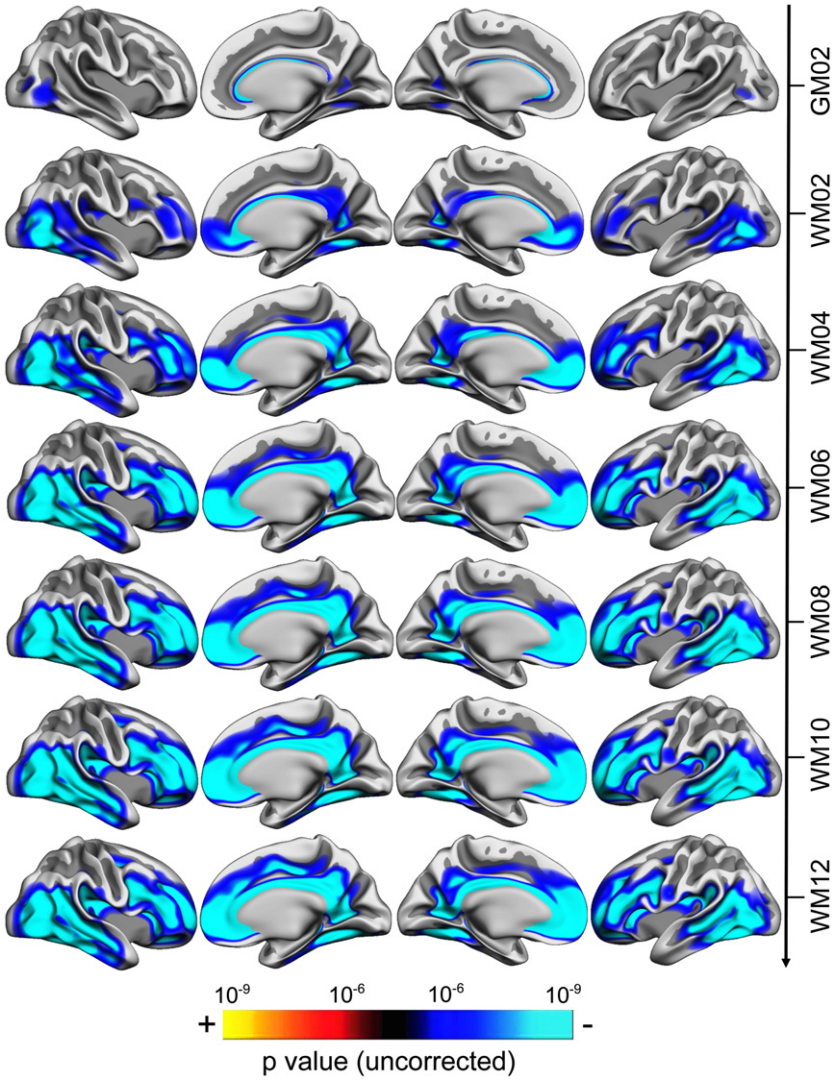

Fig. 4. Effects of age on signal intensities sampled at different distances from the WM surface. Statistical *p* maps showing the results from GLMs testing the effect of age on signal intensity mapped at six different distances from the white surface. Cold colors indicate attenuated signal with advancing age while warm color indicate the opposite relation. The statistical maps were thresholded at $p<10^{-6}$ to allow for visual inspection of regional variability over measures. Mean ventricle CSF intensity for each subject was included in the models to account for scanner related noise.

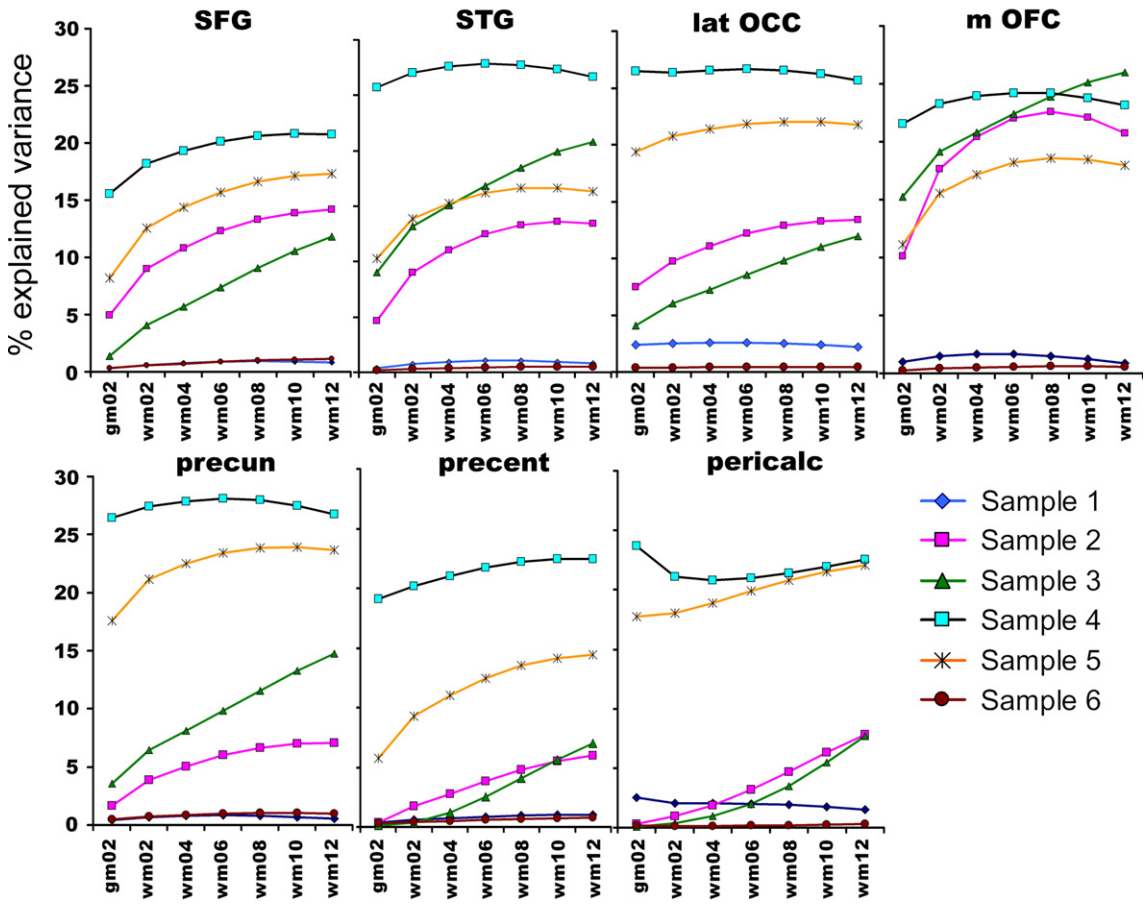

Fig. 5. Age sensitivity of signal intensity varies depending on distance from white surface and sample. The plots show percent of the variance in signal intensity explained by age (R^2) plotted as a function of sampling distance from the white surface per sample in different ROIs. SFG: superior frontal gyrus, STG: superior temporal gyrus, lat OCC: lateral occipital, m OFC, medial orbitofrontal cortex, precun: precuneus, precent: precentral, pericalc: pericalcarine.

areas. The effects were more pronounced for WM than for GM and the WM effects increased as a function of distance from the white surface. The results showed bilateral WM signal attenuation in the lateral occipital and posterior parts of the middle and inferior temporal gyri, the isthmus, precuneus and posterior cingulate gyri. Further, changes were found in large portions of the lateral frontal cortices, including rostral middle frontal gyrus, and medially in anterior parts of superior frontal and medial orbitofrontal gyri and the frontal poles. Sample related variability is displayed in Supplementary Table 5 and Fig. 5, which illustrates the amount of explained variance per sample in seven selected ROIs (superior frontal gyrus, superior temporal gyrus, lateral occipital gyrus, medial orbitofrontal cortex, precuneus, precentral and pericalcarine of the left hemisphere) at different sampling distances. Increased sampling distance from the white surface generally increased age sensitivity, levelling off at approximately 0.8 mm into the WM. Samples 2–5 showed moderate to strong relations with age in most ROIs, supporting the findings from the surface-based analyses. Signal intensity was not sensitive to age in sample 1 and 6.

Discussion

There were three main findings. First, correcting for WM/GM contrast increased both age and diagnostic sensitivity in several regions. Second, wide-spread age-related contrast decay was found, especially pronounced in frontal regions. The effects were largely overlapping with areas of cortical thinning. Third, age-related contrast decay was mainly due to decreased signal intensity in WM. The findings will be discussed below.

Increased age sensitivity after adjusting for contrast variability

Consistent age and AD related cortical thinning in samples overlapping with the current has been reported (Dickerson et al., 2009a; Fjell et al., in press). However, it has not been known to what extent these thickness effects are influenced by changes in contrast, rather than actual thickness changes per se. Further, in none of these publications have analyses on contrast or intensity parameters been conducted. Thus, the main scope of the present study is non-overlapping with the themes of the earlier reports. Regional heterogeneity of effects across the cortical mantle may be influenced by regional variability in contrast (Han et al., 2006; Jernigan et al., 2001; Raz and Rodrigue, 2006; Salat et al., 2004), but this has not been tested. Increased sensitivity for thickness changes in age and AD were found when correcting for local contrast, in general yielding both stronger and anatomically more wide-spread effects. One viable explanation is that contrast differences between subjects is a source of noise in the cortical thickness estimations, and removing this noise will yield more accurate results, thus strengthening the observed effects. Decreased contrast in elderly participants could lead to over- or underestimation of cortical thickness relative to younger participants, thereby reducing the sensitivity to real cortical thinning in aging. Likewise, non-cortical changes in AD may influence the segmentation procedures and mask actual disease related changes

in thickness. In healthy aging, both cortical thinning and contrast decay were observed over large portions of the surface, and thinning was still prominent after accounting for the shared variance between measures. Cortical thickness and tissue contrast may thus represent two distinct indices of cerebral structure, and are possibly indexing different neurobiological properties. The increase in sensitivity was replicated in the AD sample. The AD and control group were carefully matched on age, showing that the influence of tissue contrast on thickness estimates is not merely related to age-related effects. Also, the increased sensitivity for AD demonstrated that the effects of controlling for contrast differences were not merely due to between sample variability in contrast, and the procedure may thus also be used to increase the sensitivity of single-site data. More studies are needed to strengthen this finding.

The utility of the proposed correction procedure should be tested on other groups where alterations in contrast are expected. For instance, brain development is characterized by myelination of WM fibers close to the cortical mantle, thereby increasing tissue contrast on T_1-weighted images. Extrapolating the current age findings to the earliest part of the life span, an overestimation of the cortical thickness in early development is hypothesized due to decreased myelin density close to the cortical surface. This could potentially have exaggerated the reported maturational thinning from childhood through adolescence (Courchesne et al., 2000; Gogtay et al., 2004; Shaw et al., 2008; Sowell et al., 2004). Accounting for regional alterations in tissue contrast may provide improved estimates of the morphometric changes in development. More studies are needed to test this hypothesis. Cortical abnormalities have been shown in various clinical groups like Mild Cognitive Impairment (MCI) and AD (Dickerson et al., 2009a, 2009b; Fjell et al., 2008a; Im et al., 2008; Lerch et al., 2008; Seo et al., 2007; Singh et al., 2006; Thompson et al., 2007), Huntington's disease (Rosas et al., 2005, 2002, 2008), ADHD (Makris et al., 2007; Shaw et al., 2006) and Schizophrenia (Kuperberg et al., 2003; Nesvag et al., 2008). In order to increase the clinical utility of morphometric analyses, further studies should be conducted to test if the presented correction procedure also increases sensitivity in such clinical groups. This may enhance diagnostic sensitivity and thus increase the efficiency of clinical trials. Also, increased sensitivity could lead to earlier detection of progressive conditions, which could provide patients with alternative interventions and health care at an earlier stage of disease progression.

Age-related tissue contrast and WM signal decay

The tissue contrast along the WM surface diminished with advancing age, especially in frontal, lateral temporal and precuneal areas. Several factors could have contributed to this finding. It has been speculated that T_1-decay in aging is partly due to bio-accumulated iron in the cerebrum, and that this decay shows regional variability (Ogg and Steen, 1998). This underlines the importance of including vertex-wise regressors as was done in the current study. Age-related changes in T_1 may also be caused by alterations in structure and density of myelin sheaths covering the axons, primarily in WM (Koenig et al., 1990). Substantial myelin related changes in aged monkeys have been reported (Peters, 2002), including accumulation of water containing balloons in the myelin sheaths (Feldman and Peters, 1998), formation of redundant myelin, splitting of the myelin lamellae and loss of small myelinated nerve fibers (Marner et al., 2003; Sandell and Peters, 2001, 2003). Age-related changes in the architecture of myelinated neurons are known to affect the signal obtained from T_1-weighted MR sequences, with a shortening of T_1 in early development (Barkovich, 2000) and a relative lengthening of the T_1 in aging (Agartz et al., 1991; Steen et al., 1997). It has been suggested that the age-related cerebral decay mimics an inverse ontogenesis, so that the last areas to mature are the first to decline in aging and are also more vulnerable to disease (Bartzokis, 2004). The relatively strong age-related fronto-temporal gradient in contrast and signal decay observed in the present study supports this notion. The data analysed in the present study do not allow for quantitative analyses of changes in T_1, but indirectly indicate a significant lengthening of WM T_1 close to the WM surface. Although some age-related decay in GM intensity was found, the strongest effects were observed in WM resulting in reduced WM/GM contrast. In accordance with the high propensity of age-related changes in small WM nerve fibers, Tang et al. (1997) reported a 27% reduction of total length of myelinated fibers using stereological methods on human data. Further, a recent human post mortem study concluded with stronger age-related changes in WM than GM (Piguet et al., 2009) in healthy aging. Intensity analyses showed that the WM effects were larger closer to the center of the gyri relative to the tissue boundary. It is speculated that thin myelinated fibers close to the cortical mantle are especially prone to age-related decay (Bartzokis, 2004; Marner et al., 2003; Sandell and Peters, 2001, 2003). Due to methodological constraints related to image resolution and a high degree of crossing nerve fibers close to the cortical mantle, neuroimaging data supporting this hypothesis is scarce. Utilising high resolution T_1-weighted data in conjunction with a surface-based mapping procedure allowed detailed analyses not ultimately constrained by voxel resolution. The results from the present study suggest that non-pathological aging is associated with substantial T_1-lenghtening along the white surface, possibly related to changes in the density and architecture of the thin myelinated fibers intersecting the tissue boundary. The observed effects were especially pronounced in anterior portions of the brain, supporting diffusion tensor imaging (DTI) studies showing that the WM of the frontal lobe is disproportionally vulnerable to age-related alterations compared to other regions (Salat et al., 2005; Sullivan and Pfefferbaum, 2006). Further studies are needed to delineate the age-related changes in WM signal intensities to establish whether its trajectory is best explained by linear or nonlinear functions (Agartz et al., 1991).

Limitations

The present results are based on cross-sectional rather than longitudinal data. Thus, interpretations regarding continuous processes in aging and AD must be done with great caution. Further studies utilizing longitudinal data are needed to explore the aging effects on tissue contrast, and how this relates to cortical thickness estimates on an individual basis. Another limitation of the interpretation of the results is that the analysed data do not allow for detailed quantitative measurements of T_1. The T_1-weighting relative to other parameters such as proton density (PD), T_2 and T_2* varies between samples, yielding differential qualitative information available in the signal intensities. This was evident evaluating the age sensitivity of WM intensities, where two of the samples exhibited marginal age-related changes (sample 1 and 6), while the other samples showed relatively consistent age sensitivity. The datasets in sample 1 and 6 were obtained using SPGR sequences from GE scanners, while the other samples were obtained using MP-RAGE sequences on Siemens hardware, which provides much stronger T_1-weighting. In accordance with this, a recent study found high reliability of thickness estimates (i.e. tissue border classification) using non-identical but similar MP-RAGE sequences (Wonderlick et al., 2009). Although probably less pertinent to the matter of age sensitivity, another discrepancy is that there was only one acquisition in samples 1 and 6.

The results indicate that controlling for contrast increases sensitivity to age-related thickness changes across samples. This is encouraging, as it supports pooling of multiple samples and the use of legacy data in large scale multi-site studies (Fennema-Notestine et al., 2007). An inherent limitation to neuroimaging data, however, is that they do not provide direct measures of the neurobiological substrates

underlying signal intensity or morphometric properties. The cerebral effects of aging and disease progression are probably caused by a highly non-uniform collection of neurobiological perturbations (Raz and Rodrigue, 2006). The effects of age and disease on MR derived brain properties are therefore inherently dependent upon the indices collected and analysed. There are several possible causes for the observed signal decay in WM with advancing age, including accumulated iron (Jara et al., 2006; Ogg and Steen, 1998) and alterations in the architecture of myelinated axons (Barkovich, 2000, 2005). The available data do not permit excluding or favouring of any of the possible factors. Further, the same underlying neurobiological processes may cause changes in both cortical thickness and tissue contrast, and the present data does not permit us to differentiate between possible unique effects on either measure. The present surface-based segmentation procedure does unfortunately not allow for detailed mapping and analyses of possible similar intensity and contrast changes in subcortical WM/GM boundaries as observed close to the cortical surface. Further studies are therefore needed to explore the intensity and contrast dynamics in deeper structures. Another limitation is the spatial resolution of the MR images. Although the employed surface-based mapping allows morphometric inferences on a sub-millimeter scale (Dale et al., 1999; Fischl et al., 1999a; Rosas et al., 2002), the mapped intensity values are still dependent on the native resolution of the images. The volume mapping was done by weighted linear interpolations between intersecting voxels, and although this may provide a close approximation of the intensity gradient from GM to WM, it does not allow for valid inferences on a cortical laminar level.

Conclusion

The present results indicate that adjusting for local variability in tissue contrast increases cortical thickness sensitivity to AD and healthy aging. The mechanisms by which this increase is best explained are not known, but it is hypothesized that the procedure corrects for overestimations of thickness in subjects with regionally reduced tissue contrast, probably related to alterations in myelin density and water compartments close to the white surface. Further studies are needed to confirm whether employing the same correction procedure increases the diagnostic sensitivity also in other samples and in other clinical groups, thereby increasing the efficiency of clinical trials and contributing to earlier detection of progressive illnesses like AD.

Acknowledgments

The Norwegian Research Council (177404/W50) to K.B.W., (175066/D15) to A.M.F., (154313/V50) to I.R., (177458/V50) to T.E.; University of Oslo to K.B.W. and A.M.F.; the National Institutes of Health (R01-NS39581, R37-AG11230, and R01-RR13609); the Mental Illness and Neuroscience Discovery Institute; The Wallenberg Foundation and the Swedish Medical Research Council (K2004-21X-15078-01A 45, K2007-62X-15077-04-1, and K2007-62X-15078-04-3). The National Center for Research Resources (P41-RR14075, R01 RR16594-01A1 and the NCRR BIRN Morphometric Testbed BIRN002, U24 RR021382); the National Institute for Biomedical Imaging and Bioengineering (R01 EB001550, R01EB006758); the National Institute for Neurological Disorders and Stroke (R01 NS052585-01); as well as the Mental Illness and Neuroscience Discovery Institute; and is part of the National Alliance for Medical Image Computing (NAMIC), funded by the National Institutes of Health through the NIH Roadmap for Medical Research (grant U54 EB005149); additional support was provided by The Autism & Dyslexia Project funded by the Ellison Medical Foundation. We thank the developers of the OASIS (Open Access Series of Imaging Studies) database for access to MRI data constituting sample 5 and the AD and control group of the present work. *Conflict of interest*: Anders M. Dale is a founder and holds equity in CorTechs Labs, Inc., and also serves on the Scientific Advisory Board. The terms of this arrangement have been reviewed and approved by the University of California, San Diego, in accordance with its policies about conflict of interest.

Appendix A. Supplementary data

Supplementary data associated with this article can be found, in the online version, at doi:10.1016/j.neuroimage.2009.05.084.

References

Agartz, I., Saaf, J., Wahlund, L.O., Wetterberg, L., 1991. T1 and T2 relaxation time estimates in the normal human brain. Radiology 181, 537–543.
Allen, J.S., Bruss, J., Brown, C.K., Damasio, H., 2005. Normal neuroanatomical variation due to age: the major lobes and a parcellation of the temporal region. Neurobiol. Aging 26, 1245–1260 discussion 1279–1282.
Auer, S., Reisberg, B., 1997. The GDS/FAST staging system. Int. Psychogeriatr. 9 (Suppl. 1), 167–171.
Barkovich, A.J., 2000. Concepts of myelin and myelination in neuroradiology. AJNR Am. J. Neuroradiol. 21, 1099–1109.
Barkovich, A.J., 2005. Magnetic resonance techniques in the assessment of myelin and myelination. J. Inherit. Metab. Dis. 28, 311–343.
Bartzokis, G., 2004. Age-related myelin breakdown: a developmental model of cognitive decline and Alzheimer's disease. Neurobiol. Aging 25, 5–18 author reply 49–62.
Beck, A.T., Steer, R., 1987. Beck Depression Inventory Scoring Manual. The Psychological Corporation, New York.
Berg, L., 1984. Clinical Dementia Rating. Br. J. Psychiatry 145 (339).
Berg, L., 1988. Clinical Dementia Rating (CDR). Psychopharmacol. Bull. 24, 637–639.
Blessed, G., Tomlinson, B., Roth, M., 1968. The association between quantitative measures of dementia and of senile change in the cerebral grey matter of elderly subjects. Br. J. Psychiatry 114, 797–811.
Buckner, R.L., Snyder, A.Z., Shannon, B.J., LaRossa, G., Sachs, R., Fotenos, A.F., Sheline, Y.I., Klunk, W.E., Mathis, C.A., Morris, J.C., Mintun, M.A., 2005. Molecular, structural, and functional characterization of Alzheimer's disease: evidence for a relationship between default activity, amyloid, and memory. J. Neurosci. 25, 7709–7717.
Cho, S., Jones, D., Reddick, W.E., Ogg, R.J., Steen, R.G., 1997. Establishing norms for age-related changes in proton T1 of human brain tissue in vivo. Magn. Reson. Imaging 15, 1133–1143.
Cocosco, C.A., Zijdenbos, A.P., Evans, A.C., 2003. A fully automatic and robust brain MRI tissue classification method. Med. Image Anal. 7, 513–527.
Courchesne, E., Chisum, H.J., Townsend, J., Cowles, A., Covington, J., Egaas, B., Harwood, M., Hinds, S., Press, G.A., 2000. Normal brain development and aging: quantitative analysis at in vivo MR imaging in healthy volunteers. Radiology 216, 672–682.
Dale, A., Sereno, M.I., 1993. Improved localization of cortical activity by combining EEG and MEG with MRI cortical surface reconstruction: a linear approach. J. Cogn. Neurosci. 5, 162–176.
Dale, A.M., Fischl, B., Sereno, M.I., 1999. Cortical surface-based analysis. I. Segmentation and surface reconstruction. NeuroImage 9, 179–194.
de Boer, R., Vrooman, H.A., van der Lijn, F., Vernooij, M.W., Ikram, M.A., van der Lugt, A., Breteler, M.M., Niessen, W.J., 2009. White matter lesion extension to automatic brain tissue segmentation on MRI. NeuroImage 45, 1151–1161.
Desikan, R.S., Segonne, F., Fischl, B., Quinn, B.T., Dickerson, B.C., Blacker, D., Buckner, R.L., Dale, A.M., Maguire, R.P., Hyman, B.T., Albert, M.S., Killiany, R.J., 2006. An automated labeling system for subdividing the human cerebral cortex on MRI scans into gyral based regions of interest. NeuroImage 31, 968–980.
Dickerson, B.C., Bakkour, A., Salat, D.H., Feczko, E., Pacheco, J., Greve, D.N., Grodstein, F., Wright, C.I., Blacker, D., Rosas, H.D., Sperling, R.A., Atri, A., Growdon, J.H., Hyman, B.T., Morris, J.C., Fischl, B., Buckner, R.L., 2009a. The cortical signature of Alzheimer's disease: regionally specific cortical thinning relates to symptom severity in very mild to mild AD dementia and is detectable in asymptomatic amyloid-positive individuals. Cereb. Cortex 19, 497–510.
Dickerson, B.C., Feczko, E., Augustinack, J.C., Pacheco, J., Morris, J.C., Fischl, B., Buckner, R.L., 2009b. Differential effects of aging and Alzheimer's disease on medial temporal lobe cortical thickness and surface area. Neurobiol. Aging 30, 432–440.
Espeseth, T., Greenwood, P.M., Reinvang, I., Fjell, A.M., Walhovd, K.B., Westlye, L.T., Wehling, E., Lundervold, A., Rootwelt, H., Parasuraman, R., 2006. Interactive effects of APOE and CHRNA4 on attention and white matter volume in healthy middle-aged and older adults. Cogn. Affect. Behav. Neurosci. 6, 31–43.
Espeseth, T., Westlye, L.T., Fjell, A.M., Walhovd, K.B., Rootwelt, H., Reinvang, I., 2008. Accelerated age-related cortical thinning in healthy carriers of apolipoprotein E epsilon 4. Neurobiol. Aging 29, 329–340.
Feldman, M.L., Peters, A., 1998. Ballooning of myelin sheaths in normally aged macaques. J. Neurocytol. 27, 605–614.
Fennema-Notestine, C., Gamst, A.C., Quinn, B.T., Pacheco, J., Jernigan, T.L., Thal, L., Buckner, R., Killiany, R., Blacker, D., Dale, A.M., Fischl, B., Dickerson, B., Gollub, R.L., 2007. Feasibility of multi-site clinical structural neuroimaging studies of aging using legacy data. Neuroinformatics 5, 235–245.
Fischl, B., Dale, A.M., 2000. Measuring the thickness of the human cerebral cortex from magnetic resonance images. Proc. Natl. Acad. Sci. U. S. A. 97, 11050–11055.

Fischl, B., Sereno, M.I., Dale, A.M., 1999a. Cortical surface-based analysis. II: Inflation, flattening, and a surface-based coordinate system. NeuroImage 9, 195–207.
Fischl, B., Sereno, M.I., Tootell, R.B., Dale, A.M., 1999b. High-resolution intersubject averaging and a coordinate system for the cortical surface. Hum. Brain Mapp. 8, 272–284.
Fischl, B., Salat, D.H., Busa, E., Albert, M., Dieterich, M., Haselgrove, C., van der Kouwe, A., Killiany, R., Kennedy, D., Klaveness, S., Montillo, A., Makris, N., Rosen, B., Dale, A.M., 2002. Whole brain segmentation: automated labeling of neuroanatomical structures in the human brain. Neuron 33, 341–355.
Fischl, B., Salat, D.H., van der Kouwe, A.J., Makris, N., Segonne, F., Quinn, B.T., Dale, A.M., 2004a. Sequence-independent segmentation of magnetic resonance images. NeuroImage 23 (Suppl 1), S69–S84.
Fischl, B., van der Kouwe, A., Destrieux, C., Halgren, E., Segonne, F., Salat, D.H., Busa, E., Seidman, L.J., Goldstein, J., Kennedy, D., Caviness, V., Makris, N., Rosen, B., Dale, A.M., 2004b. Automatically parcellating the human cerebral cortex. Cereb. Cortex 14, 11–22.
Fjell, A.M., Walhovd, K.B., Amlien, I., Bjornerud, A., Reinvang, I., Gjerstad, L., Cappelen, T., Willoch, F., Due-Tonnessen, P., Grambaite, R., Skinningsrud, A., Stenset, V., Fladby, T., 2008a. Morphometric changes in the episodic memory network and tau pathologic features correlate with memory performance in patients with mild cognitive impairment. AJNR Am. J. Neuroradiol. 29, 1183–1189.
Fjell, A.M., Westlye, L.T., Greve, D.N., Fischl, B., Benner, T., van der Kouwe, A.J., Salat, D., Bjornerud, A., Due-Tonnessen, P., Walhovd, K.B., 2008b. The relationship between diffusion tensor imaging and volumetry as measures of white matter properties. NeuroImage 42, 1654–1668.
Fjell, A.M.,Westlye, L.T., Amlien, I., Espeseth, T., Reinvang, I., Raz, N., Agartz, I., Salat, D.H., Greve, D.N., Fischl, B., Dale, A.M., Walhovd, K.B., in press. High consistency of regional cortical thinning in aging across multiple samples. Cereb. Cortex. doi:10.1093/cercor/bhn232.
Folstein, M.F., Folstein, S.E., McHugh, P.R., 1975. "Mini-mental state". A practical method for grading the cognitive state of patients for the clinician. J. Psychiatr. Res. 12, 189–198.
Fotenos, A.F., Snyder, A.Z., Girton, L.E., Morris, J.C., Buckner, R.L., 2005. Normative estimates of cross-sectional and longitudinal brain volume decline in aging and AD. Neurology 64, 1032–1039.
Fotenos, A.F., Mintun, M.A., Snyder, A.Z., Morris, J.C., Buckner, R.L., 2008. Brain volume decline in aging: evidence for a relation between socioeconomic status, preclinical Alzheimer disease, and reserve. Arch. Neurol. 65, 113–120.
Gogtay, N., Giedd, J.N., Lusk, L., Hayashi, K.M., Greenstein, D., Vaituzis, A.C., Nugent III, T.F., Herman, D.H., Clasen, L.S., Toga, A.W., Rapoport, J.L., Thompson, P.M., 2004. Dynamic mapping of human cortical development during childhood through early adulthood. Proc. Natl. Acad. Sci. U. S. A. 101, 8174–8179.
Han, X., Jovicich, J., Salat, D., van der Kouwe, A., Quinn, B., Czanner, S., Busa, E., Pacheco, J., Albert, M., Killiany, R., Maguire, P., Rosas, D., Makris, N., Dale, A., Dickerson, B., Fischl, B., 2006. Reliability of MRI-derived measurements of human cerebral cortical thickness: the effects of field strength, scanner upgrade and manufacturer. NeuroImage 32, 180–194.
Ikram, M.A., Vrooman, H.A., Vernooij, M.W., Heijer, T.D., Hofman, A., Niessen, W.J., van der Lugt, A., Koudstaal, P.J., Breteler, M.M., in press. Brain tissue volumes in relation to cognitive function and risk of dementia. Neurobiol. Aging. doi:10.1016/j.neurobiolaging.2008.04.008.
Im, K., Lee, J.M., Seo, S.W., Yoon, U., Kim, S.T., Kim, Y.H., Kim, S.I., Na, D.L., 2008. Variations in cortical thickness with dementia severity in Alzheimer's disease. Neurosci. Lett. 436, 227–231.
Imon, Y., Yamaguchi, S., Katayama, S., Oka, M., Murata, Y., Kajima, T., Yamamura, Y., Nakamura, S., 1998. A decrease in cerebral cortex intensity on T2-weighted with ageing images of normal subjects. Neuroradiology 40, 76–80.
Jack Jr., C.R., Bernstein, M.A., Fox, N.C., Thompson, P., Alexander, G., Harvey, D., Borowski, B., Britson, P.J., J, L.W., Ward, C., Dale, A.M., Felmlee, J.P., Gunter, J.L., Hill, D.L., Killiany, R., Schuff, N., Fox-Bosetti, S., Lin, C., Studholme, C., DeCarli, C.S., Krueger, G., Ward, H.A., Metzger, G.J., Scott, K.T., Mallozzi, R., Blezek, D., Levy, J., Debbins, J.P., Fleisher, A.S., Albert, M., Green, R., Bartzokis, G., Glover, G., Mugler, J., Weiner, M.W., 2008. The Alzheimer's Disease Neuroimaging Initiative (ADNI): MRI methods. J. Magn. Reson. Imaging 27, 685–691.
Jara, H., Sakai, O., Mankal, P., Irving, R.P., Norbash, A.M., 2006. Multispectral quantitative magnetic resonance imaging of brain iron stores: a theoretical perspective. Top. Magn. Reson. Imaging 17, 19–30.
Jernigan, T.L., Archibald, S.L., Fennema-Notestine, C., Gamst, A.C., Stout, J.C., Bonner, J., Hesselink, J.R., 2001. Effects of age on tissues and regions of the cerebrum and cerebellum. Neurobiol. Aging 22, 581–594.
Jonsson, E.G., Edman-Ahlbom, B., Sillen, A., Gunnar, A., Kulle, B., Frigessi, A., Vares, M., Ekholm, B., Wode-Helgodt, B., Schumacher, J., Cichon, S., Agartz, I., Sedvall, G.C., Hall, H., Terenius, L., 2006. Brain-derived neurotrophic factor gene (BDNF) variants and schizophrenia: an association study. Prog. Neuropsychopharmacol. Biol. Psychiatry 30, 924–933.
Jovicich, J., Czanner, S., Han, X., Salat, D., van der Kouwe, A., Quinn, B., Pacheco, J., Albert, M., Killiany, R., Blacker, D., Maguire, P., Rosas, D., Makris, N., Gollub, R., Dale, A., Dickerson, B., Fischl, B., 2009. MRI-derived measurements of human subcortical, ventricular and intracranial brain volumes: reliability effects of scan sessions, acquisition sequences, data analyses, scanner upgrade, scanner vendors and field strengths. NeuroImage 46 (1), 177–192.
Koenig, S.H., Brown III, R.D., Spiller, M., Lundbom, N., 1990. Relaxometry of brain: why white matter appears bright in MRI. Magn. Reson. Med. 14, 482–495.
Kuperberg, G.R., Broome, M.R., McGuire, P.K., David, A.S., Eddy, M., Ozawa, F., Goff, D., West, W.C., Williams, S.C., van der Kouwe, A.J., Salat, D.H., Dale, A.M., Fischl, B., 2003. Regionally localized thinning of the cerebral cortex in schizophrenia. Arch. Gen. Psychiatry 60, 878–888.
Lerch, J.P., Pruessner, J., Zijdenbos, A.P., Collins, D.L., Teipel, S.J., Hampel, H., Evans, A.C., 2008. Automated cortical thickness measurements from MRI can accurately separate Alzheimer's patients from normal elderly controls. Neurobiol. Aging 29, 23–30.
Makris, N., Biederman, J., Valera, E.M., Bush, G., Kaiser, J., Kennedy, D.N., Caviness, V.S., Faraone, S.V., Seidman, L.J., 2007. Cortical thinning of the attention and executive function networks in adults with attention-deficit/hyperactivity disorder. Cereb. Cortex 17, 1364–1375.
Marcus, D.S., Wang, T.H., Parker, J., Csernansky, J.G., Morris, J.C., Buckner, R.L., 2007. Open Access Series of Imaging Studies (OASIS): cross-sectional MRI data in young, middle aged, nondemented, and demented older adults. J. Cogn. Neurosci. 19, 1498–1507.
Marner, L., Nyengaard, J.R., Tang, Y., Pakkenberg, B., 2003. Marked loss of myelinated nerve fibers in the human brain with age. J. Comp. Neurol. 462, 144–152.
Morris, J.C., 1993. The Clinical Dementia Rating (CDR): current version and scoring rules. Neurology 43, 2412–2414.
Nesvag, R., Lawyer, G., Varnas, K., Fjell, A.M., Walhovd, K.B., Frigessi, A., Jonsson, E.G., Agartz, I., 2008. Regional thinning of the cerebral cortex in schizophrenia: effects of diagnosis, age and antipsychotic medication. Schizophr. Res. 98, 16–28.
Ogg, R.J., Steen, R.G., 1998. Age-related changes in brain T1 are correlated with iron concentration. Magn. Reson. Med. 40, 749–753.
Pakkenberg, B., Gundersen, H.J., 1997. Neocortical neuron number in humans: effect of sex and age. J. Comp. Neurol. 384, 312–320.
Pardoe, H., Pell, G.S., Abbott, D.F., Berg, A.T., Jackson, G.D., 2008. Multi-site voxel-based morphometry: methods and a feasibility demonstration with childhood absence epilepsy. NeuroImage 42, 611–616.
Peters, A., 2002. The effects of normal aging on myelin and nerve fibers: a review. J. Neurocytol. 31, 581–593.
Piguet, O., Double, K., Kril, J., Harasty, J., Macdonald, V., McRitchie, D., Halliday, G., 2009. White matter loss in healthy aging: A postmortem study. Neurobiol Aging.
Raz, N., Rodrigue, K.M., 2006. Differential aging of the brain: patterns, cognitive correlates and modifiers. Neurosci. Biobehav. Rev. 30, 730–748.
Raz, N., Millman, D., Sarpel, G., 1990. Cerebral correlates of cognitive aging: Gray-white-matter differentiation in the medial temporal lobes, and fluid versus crystallized abilities. Psychobiology 18, 475–481.
Raz, N., Gunning-Dixon, F., Head, D., Rodrigue, K.M., Williamson, A., Acker, J.D., 2004a. Aging, sexual dimorphism, and hemispheric asymmetry of the cerebral cortex: replicability of regional differences in volume. Neurobiol. Aging 25, 377–396.
Raz, N., Rodrigue, K.M., Head, D., Kennedy, K.M., Acker, J.D., 2004b. Differential aging of the medial temporal lobe: a study of a five-year change. Neurology 62, 433–438.
Raz, N., Lindenberger, U., Rodrigue, K.M., Kennedy, K.M., Head, D., Williamson, A., Dahle, C., Gerstorf, D., Acker, J.D., 2005. Regional brain changes in aging healthy adults: general trends, individual differences and modifiers. Cereb. Cortex 15, 1676–1689.
Resnick, S.M., Goldszal, A.F., Davatzikos, C., Golski, S., Kraut, M.A., Metter, E.J., Bryan, R.N., Zonderman, A.B., 2000. One-year age changes in MRI brain volumes in older adults. Cereb. Cortex 10, 464–472.
Resnick, S.M., Pham, D.L., Kraut, M.A., Zonderman, A.B., Davatzikos, C., 2003. Longitudinal magnetic resonance imaging studies of older adults: a shrinking brain. J. Neurosci. 23, 3295–3301.
Rosas, H.D., Liu, A.K., Hersch, S., Glessner, M., Ferrante, R.J., Salat, D.H., van der Kouwe, A., Jenkins, B.G., Dale, A.M., Fischl, B., 2002. Regional and progressive thinning of the cortical ribbon in Huntington's disease. Neurology 58, 695–701.
Rosas, H.D., Hevelone, N.D., Zaleta, A.K., Greve, D.N., Salat, D.H., Fischl, B., 2005. Regional cortical thinning in preclinical Huntington disease and its relationship to cognition. Neurology 65, 745–747.
Rosas, H.D., Salat, D.H., Lee, S.Y., Zaleta, A.K., Pappu, V., Fischl, B., Greve, D., Hevelone, N., Hersch, S.M., 2008. Cerebral cortex and the clinical expression of Huntington's disease: complexity and heterogeneity. Brain 131, 1057–1068.
Salat, D.H., Buckner, R.L., Snyder, A.Z., Greve, D.N., Desikan, R.S., Busa, E., Morris, J.C., Dale, A.M., Fischl, B., 2004. Thinning of the cerebral cortex in aging. Cereb. Cortex 14, 721–730.
Salat, D.H., Tuch, D.S., Hevelone, N.D., Fischl, B., Corkin, S., Rosas, H.D., Dale, A.M., 2005. Age-related changes in prefrontal white matter measured by diffusion tensor imaging. Ann. N.Y. Acad. Sci. 1064, 37–49.
Salat, D.H., Greve, D.N., Pacheco, J.L., Quinn, B.T., Helmer, K.G., Buckner, R.L., Fischl, B., 2009. Regional white matter volume differences in nondemented aging and Alzheimer's disease. NeuroImage 44, 1247–1258.
Sandell, J.H., Peters, A., 2001. Effects of age on nerve fibers in the rhesus monkey optic nerve. J. Comp. Neurol. 429, 541–553.
Sandell, J.H., Peters, A., 2003. Disrupted myelin and axon loss in the anterior commissure of the aged rhesus monkey. J. Comp. Neurol. 466, 14–30.
Segonne, F., Dale, A.M., Busa, E., Glessner, M., Salat, D., Hahn, H.K., Fischl, B., 2004. A hybrid approach to the skull stripping problem in MRI. NeuroImage 22, 1060–1075.
Segonne, F., Grimson, E., Fischl, B., 2005. A genetic algorithm for the topology correction of cortical surfaces. Inf. Process. Med. Imag. 19, 393–405.
Segonne, F., Pacheco, J., Fischl, B., 2007. Geometrically accurate topology-correction of cortical surfaces using nonseparating loops. IEEE Trans. Med. Imag. 26, 518–529.
Seo, S.W., Im, K., Lee, J.M., Kim, Y.H., Kim, S.T., Kim, S.Y., Yang, D.W., Kim, S.I., Cho, Y.S., Na, D.L., 2007. Cortical thickness in single- versus multiple-domain amnestic mild cognitive impairment. NeuroImage 36, 289–297.
Shaw, P., Lerch, J., Greenstein, D., Sharp, W., Clasen, L., Evans, A., Giedd, J., Castellanos, F.X., Rapoport, J., 2006. Longitudinal mapping of cortical thickness and clinical outcome in children and adolescents with attention-deficit/hyperactivity disorder. Arch. Gen. Psychiatry 63, 540–549.
Shaw, P., Kabani, N.J., Lerch, J.P., Eckstrand, K., Lenroot, R., Gogtay, N., Greenstein, D., Clasen, L., Evans, A., Rapoport, J.L., Giedd, J.N., Wise, S.P., 2008. Neurodevelopmental trajectories of the human cerebral cortex. J. Neurosci. 28, 3586–3594.

Singh, V., Chertkow, H., Lerch, J.P., Evans, A.C., Dorr, A.E., Kabani, N.J., 2006. Spatial patterns of cortical thinning in mild cognitive impairment and Alzheimer's disease. Brain 129, 2885–2893.

Sowell, E.R., Peterson, B.S., Thompson, P.M., Welcome, S.E., Henkenius, A.L., Toga, A.W., 2003. Mapping cortical change across the human life span. Nat. Neurosci. 6, 309–315.

Sowell, E.R., Thompson, P.M., Leonard, C.M., Welcome, S.E., Kan, E., Toga, A.W., 2004. Longitudinal mapping of cortical thickness and brain growth in normal children. J. Neurosci. 24, 8223–8231.

Steen, R.G., Ogg, R.J., Reddick, W.E., Kingsley, P.B., 1997. Age-related changes in the pediatric brain: quantitative MR evidence of maturational changes during adolescence. AJNR Am. J. Neuroradiol. 18, 819–828.

Sullivan, E.V., Pfefferbaum, A., 2006. Diffusion tensor imaging and aging. Neurosci. Biobehav. Rev. 30, 749–761.

Tang, Y., Nyengaard, J.R., Pakkenberg, B., Gundersen, H.J., 1997. Age-induced white matter changes in the human brain: a stereological investigation. Neurobiol. Aging 18, 609–615.

Thompson, P.M., Hayashi, K.M., Sowell, E.R., Gogtay, N., Giedd, J.N., Rapoport, J.L., de Zubicaray, G.I., Janke, A.L., Rose, S.E., Semple, J., Doddrell, D.M., Wang, Y., van Erp, T.G., Cannon, T.D., Toga, A.W., 2004. Mapping cortical change in Alzheimer's disease, brain development, and schizophrenia. NeuroImage 23 (Suppl. 1), S2–18.

Thompson, P.M., Hayashi, K.M., Dutton, R.A., Chiang, M.C., Leow, A.D., Sowell, E.R., De Zubicaray, G., Becker, J.T., Lopez, O.L., Aizenstein, H.J., Toga, A.W., 2007. Tracking Alzheimer's disease. Ann. N.Y. Acad. Sci. 1097, 183–214.

Vrooman, H.A., Cocosco, C.A., van der Lijn, F., Stokking, R., Ikram, M.A., Vernooij, M. W., Breteler, M.M., Niessen, W.J., 2007. Multi-spectral brain tissue segmentation using automatically trained k-Nearest-Neighbor classification. NeuroImage 37, 71–81.

Walhovd, K.B., Fjell, A.M., Reinvang, I., Lundervold, A., Dale, A.M., Eilertsen, D.E., Quinn, B.T., Salat, D., Makris, N., Fischl, B., 2005. Effects of age on volumes of cortex, white matter and subcortical structures. Neurobiol. Aging 26, 1261–1270 discussion 1275–1268.

Walhovd, K.B., Fjell, A.M., Dale, A.M., McEvoy, L.K., Brewer, J., Karow, D.S., Salmon, D.P., Fennema-Notestine, C., in press-a. Multi-modal imaging predicts memory performance in normal aging and cognitive decline. Neurobiol. Aging. doi:10.1016/j.neurobiolaging.2008.08.013.

Walhovd, K.B., Fjell, A.M., Amlien, I., Grambaite, R., Stenset, V., Bjornerud, A., Reinvang, I., Gjerstad, L., Cappelen, T., Due-Tonnessen, P., Fladby, T., 2009a. Multimodal imaging in mild cognitive impairment: metabolism, morphometry and diffusion of the temporal-parietal memory network. NeuroImage 45, 215–223.

Walhovd, K.B.,Westlye, L.T., Amlien, I., Espeseth, T., Reinvang, I., Raz, N., Agartz, I., Salat, D., Greve, D.N., Fischl, B., Dale, A.M., Fjell, A.M., in press-b. Consistent neuroanatomical age-related volume differences across multiple samples. Neurobiol. Aging.

Wechsler, D., 1999. Wechsler Abbreviated Scale of Intelligence. The Psychological Corporation, San Antonio, TX.

Westlye, L.T., Walhovd, K.B., Bjornerud, A., Due-Tonnessen, P., Fjell, A.M., 2009. Error-related negativity is mediated by fractional anisotropy in the posterior cingulate gyrus — a study combining diffusion tensor imaging and electrophysiology in healthy adults. Cereb. Cortex 19, 293–304.

Wonderlick, J.S., Ziegler, D.A., Hosseini-Varnamkhasti, P., Locascio, J.J., Bakkour, A., van der Kouwe, A., Triantafyllou, C., Corkin, S., Dickerson, B.C., 2009. Reliability of MRI-derived cortical and subcortical morphometric measures: effects of pulse sequence, voxel geometry, and parallel imaging. NeuroImage 44, 1324–1333.